



FLASH FLOOD HAZARD MAPPING OF WADI BABA BASIN, SOUTHWESTERN SINAI, EGYPT

Ali E. Omar^{*1}, M.O. Arnous², M.A. El-Ghawaby², A.S. Alshami¹
and M.A. El Zalaky¹

1. Dept. Geol. and Remote Sensing, Authority of Nuclear Materials, Egypt

2. Dept. Geol., Fac. Sci., Suez Canal Univ., Egypt

ABSTRACT

Flash flood hazard in the mountainous area of Southwestern Sinai demands reliable and accurate information. Flash flood is the mainly dangerous hazard to spotlight on because it threatens the life of people and retards any sustainable development planning in and around the rugged topography areas. The current study aims to applying GIS and remote sensing tools to construct flash flood hazards map based on geomorphometric parameters extracted from Digital Elevation Model (DEM) and assess the flash flood hazard risk rank for W. Baba basin and its sub-basins. Wadi Baba is located in an arid region and is considered as a significant basin in Southwestern Sinai area (SWSA) that drains into the Gulf of Suez. The drainage networks and basin boundary were delineated and morphometric parameters of the drainage system were calculated. The flood intensity is controlled mainly by values of geomorphometric parameters, soil and geological characteristics, and the meteorological conditions. The analysis of the various morphometric parameters of the W. Baba shows that they have different impacts on the flash flood intensity. Depending on the statistically computed weights and mean values of the important geomorphometric parameters and then integrated by using GIS functions; the sub-basins of W. Baba are classified into three categorized risk wise, namely: high, moderate and low flash flood hazard. The sub-basins which have high flash flood hazard rank with low probability of ground water recharge are geospatially mapped.

Key words: GIS, Flash floods, Hazard mapping, Sinai, Basin morphometry.

INTRODUCTION

Natural hazards are cyclic natural phenomena that threaten lives, property, and assets. Flash flood is considered as one of the major dangerous events in the world often occur in arid regions reasoning the greatest amount of losses of life and property damage (CEOS 2003; Arnous *et al.*, 2011; Subyani 2011; Arnous and Green 2011).

Today, the space-born remote sensing data, besides Geographic Information Systems (GIS), recommends an outstanding different

to predictable tool in assessing, integrating, and mapping different types of natural hazard events. There are several studies has been published around the world to illustrate how to apply the remote sensing and GIS techniques for the hydrometrological hazards investigations, mapping and mitigation measures particularly for the sustainable development in arid regions (Zerger and Smith 2003; Bapalu and Sinha 2005; Fernandez and Lutz 2010; Arnous, 2011, Arnous *et al.*, 2011, Omran *et al.*, 2011; Arnous and Green 2011, Abd Manap *et al.*, 2013; Bajabaa *et al.*, 2014; Arnous and Green 2015; Arnous *et al.*

* Corresponding author: Tel.: +20100992307

E-mail address: aliomarnma@gmail.com

2015). The drainage network characteristics in numerous arid zones of the world have been investigated by applying the principals of the geomorphological approaches mainly based on the **Horton (1945) and Strahler (1964)**. The morphometric characteristics of the network that are extracted from the Remote Sensing digital data have been used to estimate, describe, assess, predict and identify the relationships between the morphometric parameters of the basin and flash flood risk and their environmental impacts (**Patton 1988, Gardiner 1990; Nageswararao *et al.* 2010; Arnous *et al.*, 2011**).

South Sinai region, is characterized by its, rugged topography and high mountains landscape, which identified as a flood prone area where flash floods are recorded frequently and resulted in significant infrastructure damages, population displacement and sometimes loss of lives. Most of the flood management strategies in this area have been geared towards preventing flood by dams construction. Actually, these dams capacity are not sufficient to cover the 100 years return period rainfall and very little attention is paid for land use planning to reduce the risk of flood disasters. The geomorphology and geology of the SWSA has been studied by several authors such as **Ball (1916), Shata (1955), Hammad (1980), Saad *et al.* (1980), El-Shamy (1983), Hammad and Misak (1985), Aglan (1995), Aggour and Gomaa (2008), El-Rayes and Arnous (2015), El-Rayes *et al.* (2015)**. In addition, the precipitation in the SWSA takes place during autumn, winter and spring with long dry summer.

The SWSA may subjected to separate dry climate for several successive years. The rain storms of high rate and short duration may take place once every three or four years causing torrential floods (**El Shamy, 1983**). The evaluation and assessment of flood hazard impacts need more detailed information of climatic and

hydrogeological conditions including rainfall data and evaporation processes, topographic and geomorphological information including wadi borders types and their drainage systems. The integration of these factors on flooding predictions and estimation in different environmental countries have been carried out by many case studies (**Al-Harthi, 2003**).

The current work is an attempt to analyze, evaluate and assess the flood hazard potentiality of the W. Baba basin based on remote sensing and GIS tools. To accomplish these intents, it was necessary to perform the identification of the climatic conditions of the adjoining region. Recognizing the effects of topography, lithology and geological structures of the basin system on flood intensity are performed.

Study Area

The area of study is situated in southwestern Sinai, to the east of Abu Zenima city between Longitudes 33° 05' and 33° 34' E and Latitudes 28° 52' and 29° 05' N (Fig. 1), and covers an area of about 3100 km². It is covered by a sedimentary succession of Cambro-Ordovician, Lower Carboniferous, Cretaceous and Quaternary ages overlying the Proterozoic granitic rocks that have an age of 591±6 Ma (**Be'eri-Shlevin *et al.*, 2009; Eyal *et al.*, 2010**) and involved within the northern part of the Arabo-Nubian crystalline massif.

The climatic regime of the study area recognized based on the records of seven meteorological stations located at Ras Sudr, Nekhel, Ras El-Naqb, Abu Rudies, Saint Catherine, El-Tor and Sharm El-Sheikh. The measured meteorological elements were collected from both Climatological Normals of The **Arab Republic of Egypt (1980) and Climatic Atlas of Egypt (1996)** (Table 1). Sinai Peninsula belongs to an area lying within the arid belt. It has low precipitation, high evaporation and temperature with hot long summer and mild short winter.

The study area receives occasionally heavy rain storms every two or four years (**El Shamy, 1983**) causing catastrophic floods that runs downhill towards the Gulf of Suez. The climatic parameters (temperature, relative humidity, surface wind and rainfall) have a great effect on floods and groundwater recharge, in addition to its role on topographic sculpturing which creates different geomorphic units of the area. Based on the available meteorological data that collected from pre-mentioned stations, and isohyetal contour maps of southern Sinai; the average rainfall intensities digital map is established (Fig. 2).

MATERIALS AND METHODS

The available data is employed to assess the flash flood hazards are mainly represented in Remote sensing data; which include the Landsat 7 (ETM) and Landsat 8 (OLI) dated 2005 and 2013 respectively. Furthermore, ASTER GDEM data are used to carry out terrain analysis and to detect the geologic, topographic and geomorphologic characteristics of the study area. The GDEM of the study area used to construct slope, slope aspect, hill-shade, drainage lines and catchment area of W. Baba network basin. GIS tools area used to delineate and extract the stream networks and to assess and manage the flash flood hazard (**Maidment 2002; Zhang et al., 2009; Omran et al. 2011, Arnous 2016**).

Based mainly on utilizing the Arc Hydro tools in spatial analyst of ARC GIS, the morphometric parameters of Wadi Baba basin in Sinai are extracted and mapped the watershed area. The morphometric parameters results were extracted automatically using based mainly on Arc Hydro functions such as fill Sinks, flow direction, stream definition, stream segmentation and stream order (**Kumar et al., 2000; Zhang et al., 2009; Omran, 2011; Rai et al., 2014; Arnous 2016**).

The stream network is extracted from the GDEM to prepare and create the stream network and ordering maps of the study area. Stream ordering is the mean of conveying a numeric order to relatives in the stream basin network. In the current work, Strahler method is used to ordering system of the Baba basin that are assigning as the sixth order network basin.

The results were verified and standardized by evaluating those with rectified topographic maps of W. Baba basin. The delineation of basin boundaries is created by using watershed tools to identify the water divide between sub-basins and also to guarantee the choice of points of high accumulated flow during delineation drainage basins (**Omran et al., 2011**).

The results of this process provided and delineated the sub-basins in the study area that were then categorized depending mainly on their size of the watershed, total length and number of segments for each stream order of basin. The morphometric parameters were calculated, and estimated from the analysis of various drainage elements, such as ordering of the different streams, basin area and perimeter and length of drainage channels, basin ratio, stream frequency, drainage texture ratio, elongation ratio, circularity index, drainage density in addition to the bifurcation ratio (**Martz and Garbreche, 1992; Kumar et al., 2000; Arnous et al., 2011; Omran et al., 2011; Mondal and Gupta, 2015**). Finally, the statistical analysis of the commutative weights morphometric parameters data is integrated by using GIS. The flash flood vulnerable sites has been identified and relatively categorized, risk-wise ranks, into three orders, namely: high, moderate and low.

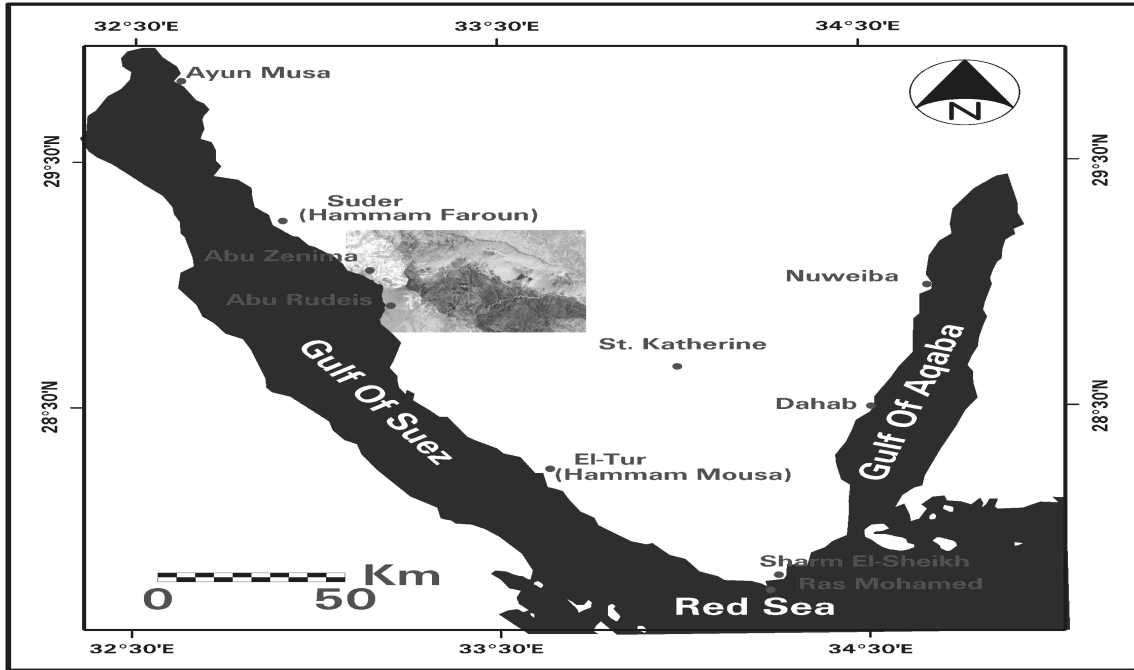


Fig. (1): location map of the study area.

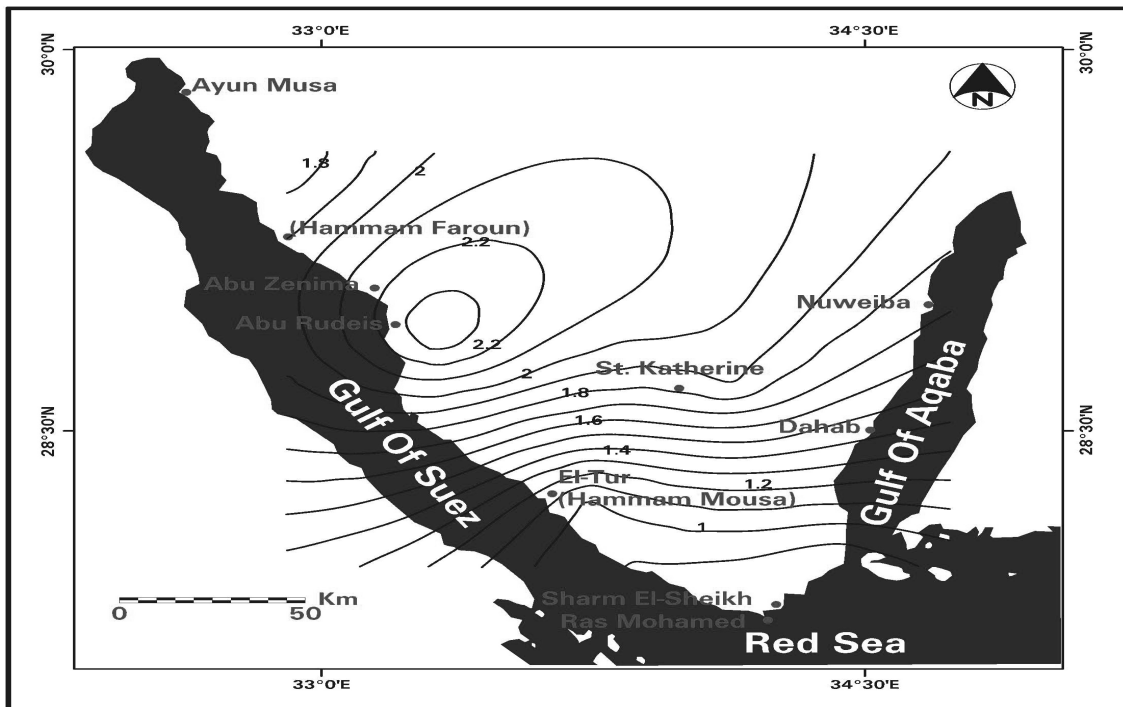


Fig. (2): Average rainfall intensities over South Sinai Peninsula (average of the period from 1961-1990), after Saad et al. (1980) values in mm/y.

Table (1): The meteorological data of some stations in Southern SINAI.

Station	Record years	Measured elements	Jan.	Feb.	Mar.	Apr.	May.	Jun.	Jul.	Aug.	Sep.	Oct.	Nov.	Dec.	Total	Annual mean
Ras Sudr	(1961-1990)	R.H.%	55	55	55	55	55	55	55	55	65	65	65	65	700	58.3
		Max.T.C°	17.5	22.5	22.5	27.5	32.5	32.5	37.5	32.5	32.5	27.5	27.5	22.5	335	27.9
		Min.T.C°	7.5	7.5	12.5	12.5	17.5	22.5	22.5	22.5	22.5	17.5	12.5	12.5	190	15.8
		R.F. mm	3.5	3.5	3.5	1	1	1	0	0	1	1	1	3.5	20	1.7
Nekhel	(1962-1967)	R.H.%	62	50	51	44	44	41	46	50	59	61	61	59	628	52.3
		Max.T.C°	17.7	19.3	20.4	27.4	30.6	34.4	35.4	35.3	31.8	29.2	23.6	19.5	325	27.1
		Min.T.C°	2.1	2.9	4.9	8.8	11.5	14.5	16.4	17.1	15.2	12.3	8.4	3.7	118	9.8
		R.F. mm	10.3	6.6	3.3	1.4	Tr.	Tr.	0	0	Tr.	3.8	7.6	5.2	38.2	4.2
Ras El-Naqb	(1961-1990)	Evap.mm	5.6	7.1	10.4	13.1	15.5	17.5	16.7	14.7	12.2	10.6	7.2	5.9	137	11.4
		R.H.%	55	45	45	35	35	35	45	45	45	45	45	55	530	44.2
		Max.T.C°	17.5	17.5	22.5	27.5	32.5	32.5	32.5	32.5	32.5	27.5	22.5	17.5	315	26.4
		Min.T.C°	2.5	2.5	7.5	12.5	12.5	17.5	22.5	17.5	17.5	12.5	7.5	7.5	140	11.7
Abu Rudies	(1961-1990)	R.F. mm	3.5	3.5	3.5	1	1	1	0	0	1	1	3.5	3.5	22.5	1.9
		R.H.%	56	55	54	54	55	55	57	57	58.5	58	56.5	56.5	673	56
		Max.T.C°	21.7	21.8	23.3	27.2	30.1	32.1	32.4	32.8	31.7	28.6	27.1	22.6	331	27.6
		Min.T.C°	9.25	12.4	13.4	17.6	21.7	23.3	23.9	27	23.7	22.2	17.4	12.6	224	18.7
St. Catherine	(1937-1943)	R.F. mm	4.15	1	0.6	0.6	Tr.	0.5	0	0	0.5	0.62	1.15	20.2	29.4	2.4
		Evap.mm	7.7	8.3	9.3	10.2	11.3	12	11.2	12	11.7	10.2	8.3	7.8	120	10
		R.H.%	28	30	20	17	23	18	23	22	17	30	40	36	304	25.3
		Max.T.C°	-11	12.3	20.6	23.1	24.6	24.8	24.7	25.8	25.8	21.9	17.2	12.4	222	18.5
EL-Tor	(1919-1967)	Min.T.C°	-15	-14	-5.3	-4.6	0.3	3.9	7.9	6.6	5.3	1.9	-0.2	-8.9	-23.4	-2.0
		R.F. mm	1.5	1.4	10	7.9	6	Tr.	0	0	0	4.6	22	7	60.4	5.5
		R.H.%	45	35	35	25	25	25	25	25	25	25	35	35	360	30.0
		Max.T.C°	12.5	12.5	17.5	22.5	27.5	32.5	32.5	32.5	32.5	27.5	17.5	17.5	285	23.8
Sharm El-Sheikh	(1961-1990)	Min.T.C°	2.5	2.5	7.5	12.5	17.5	17.5	17.5	17.5	17.5	12.5	7.5	2.5	135	11.3
		R.F. mm	3.5	3.5	3.5	3.5	1	1	0	0	1	1	1	3.5	22.5	1.9
		R.H.%	57	55	53	56	85	59	60	61	63	58	58	56	721	60.1
		Max.T.C°	21.1	21.7	24.2	27.9	30.7	33.5	34.6	34.8	32.6	29.6	26.6	22.5	340	28.3
Sharm El-Sheikh	(1955_1955)	Min.T.C°	9	9.7	12.6	16.5	20.5	23.3	24.5	23.8	22.8	18.5	14.7	10.8	207	17.2
		R.F. mm	1.5	1.3	1.2	0.2	0.2	Tr.	0	0	0	0.7	1.7	3.6	10.4	0.9
		Evap.mm	7	7.8	9.2	10.2	11.1	12.5	11.9	11.8	10.4	8	7.4	7	114	9.5
		R.H.%	55	55	55	55	55	55	55	55	65	55	55	55	670	55.8
Sharm El-Sheikh	(1961-1990)	Max.T.C°	22.5	22.5	22.5	27.5	32.5	32.5	37.5	32.5	32.5	27.5	27.5	22.5	340	28.3
		Min.T.C°	12.5	12.5	12.5	17.5	22.5	22.5	22.5	27.5	22.5	17.5	17.5	12.5	220	18.3
		R.F. mm	1	1	1	1	1	1	0	0	1	1	1	3.5	12.5	1.0
		R.H.%	52	41	41	42	36	38	38	52	48	44	46	50	528	44.0
Sharm El-Sheikh	(1955_1955)	Max.T.C°	23.4	25.7	25.6	28.9	32.8	35.8	35.7	34.2	34.4	33.1	27.6	22.7	360	30.0
		Min.T.C°	15.8	16.6	17.7	20.7	24.1	26.1	26.7	26.6	26	22.8	20	15.9	259	21.6
		R.F. mm	0.2	0	0	0.2	Tr.	0	0	0	0	0	0	23.4	23.8	2.2
		R.H.%	45	45	45	35	35	35	35	35	45	45	45	45	490	40.8
Sharm El-Sheikh	(1961-1990)	Max.T.C°	22.5	22.5	27.5	27.5	32.5	37.5	37.5	37.5	32.5	27.5	27.5	22.5	355	29.6
		Min.T.C°	12.5	12.5	17.5	17.5	22.5	27.5	27.5	27.5	27.5	22.5	17.5	12.5	245	20.4
		R.F. mm	1	1	1	1	1	1	0	0	1	1	1	1	10	0.8

LEGEND:

R.H.% = Relative humidity.

Max.T.C° = Maximum air temperature.

Min.T.C° = Minimum air temperature.

R.F. = Rainfall (mm)

Evap. = Evaporation (mm)

Tr. = Trace (less than 0.1 mm).

0 = precipitation is rare during corresponding months.

RESULTS AND DISCUSSION

The integrated results of the satellite remote sensing and GIS data are used for assessing and mapping the flood hazard as discussed in the following sections:

Hydrographic Basins

The drainage system in any area reveals to differing degrees the natures of lithology and structures. It depends mainly on the type, distribution and attitude of the surface rocks, bedding planes, joints, faults and folds.

Moreover, the drainage pattern depends on the climate conditions as rainfall and temperature. The drainage networks of W. Baba basin are internal and external, well developed, and highly integrated. To get these maps for the basin catchment area and drainage pattern networks, a tracing of the drainage networks from the GDEM is extracted from ASTER satellite image by using Arc GIS software program. The produced maps by this technique include basin boundaries and drainage network maps. The hydrographic basins of the study area are running in general ENE to WSW direction. The main trunk of the wadi open into the coastal plain and spread out like a delta to reach the Gulf of Suez by numerous very shallow channels forming El Markha Plain.

W. Baba hydrographic basin drains into the Gulf of Suez at about 9 km to the north of Abu Rudies Town. It has surface area of about 688.3 km², length of about 56 km long and basin perimeter of about 194.8 km (Fig. 3). W. Baba hydrographic basins drains several tributaries at the upstreams due the northeast.

The upstream part draining El Tih southern escarpment by W. El Garf and W. Rowekta sub-basins, which are characterized by wide channels. W. Baba extends westward forming W. El Sih. Rocks of this part are mainly friable sandstone. The middle part that goes through hard igneous and metamorphic rocks is characterized by a narrow channel with several meanders. The downstream parts, which mostly covered by low sedimentary hilly terrain, is characterized by a relatively wide channel with gentle slope.

Basin Morphometry

Remote sensing and GIS data analysis and interpretation are a very useful in the geomorphological mapping and detection of the verified reserves of groundwater (El-Baz, 1995; Arnous, 2016). The morphometric analysis of W. Baba drainage basin had been carefully studied. The drainage network of Baba basin is extracted, delineated and verified on correctly enhanced digital remote sensing data by using Arc Hydro tools and visual interpretation. The hydrographic basin of W. Baba is delineated and divided into 23 sub-basins. Morphometric parameters of the drainage network were also computed using interactivity Arc GIS and ERDAS imagine software programs.

The morphometric parameters including the stream order (U), bifurcation ratio (Rb), stream frequency (F), stream density (D), and other morphometric parameters are listed in Table 2. The watersheds of the W. Baba basin are classified relative to their geomorphological characteristics for each watershed.

W. Baba covers an area of about 688.3 km² with 56 km long. Basin perimeter is about 194.8 km, bifurcation ratio is 4.58, weighted mean bifurcation ratio is 1.19, drainage frequency is 3.32, drainage density is 2.19, overland flow is 0.229 and the shape of the basin have circularity ratio of 0.228 and elongation ratio of 0.539. It drains watershed area with slope gradient of about 20.63 m/km from G. El-Tih with heights between 979 m and 1152 m from the north and from a small part of G. Raqaba with heights between 1265 m and 1396 m from the northeast. It drains the westward area passing through a wide sandy area called Ramlet Hemeiyir, then southwestward passing with Um Bogma area, then to west Baba delta and finally to the Gulf of Suez at Ras Abu Rudies. W. Baba has sixth order trunk that reflects the wide areal extent of the basin (Table 3). In the present study, W. Baba is divided into twenty-three (23) relatively large sub-basins (Fig. 4 and Table 3).

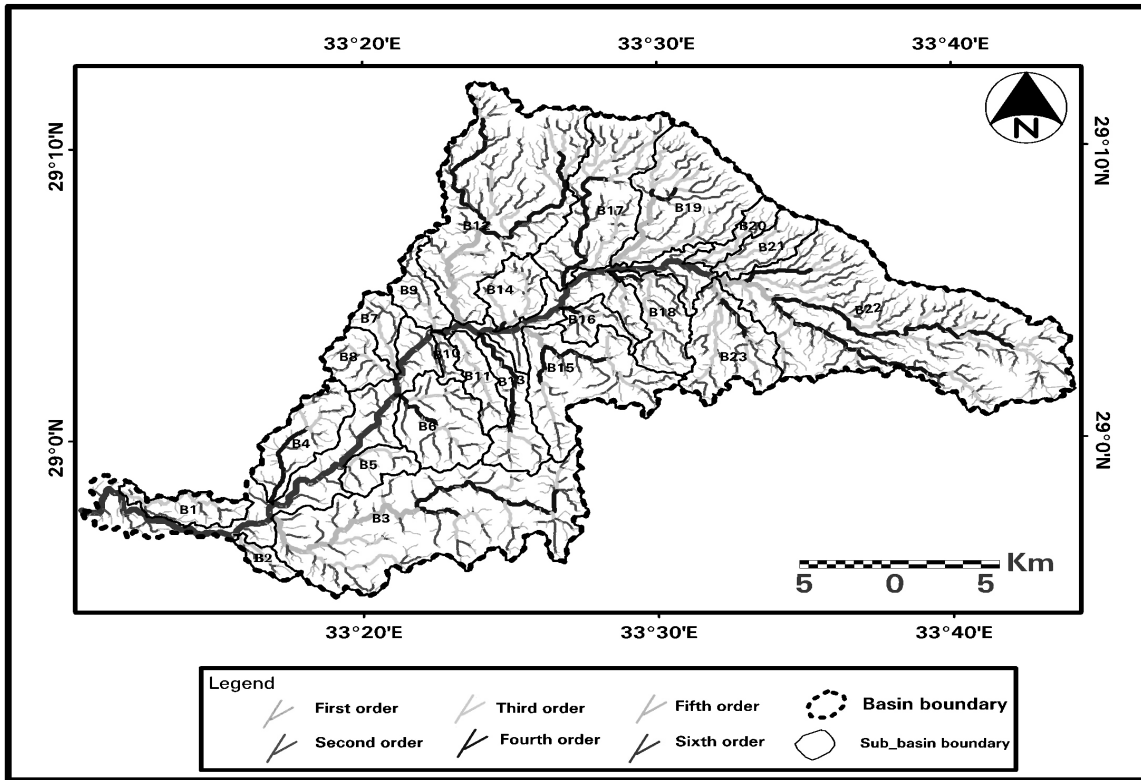


Fig. (3): Drainage network of Wadi Baba basin and related sub-basins.

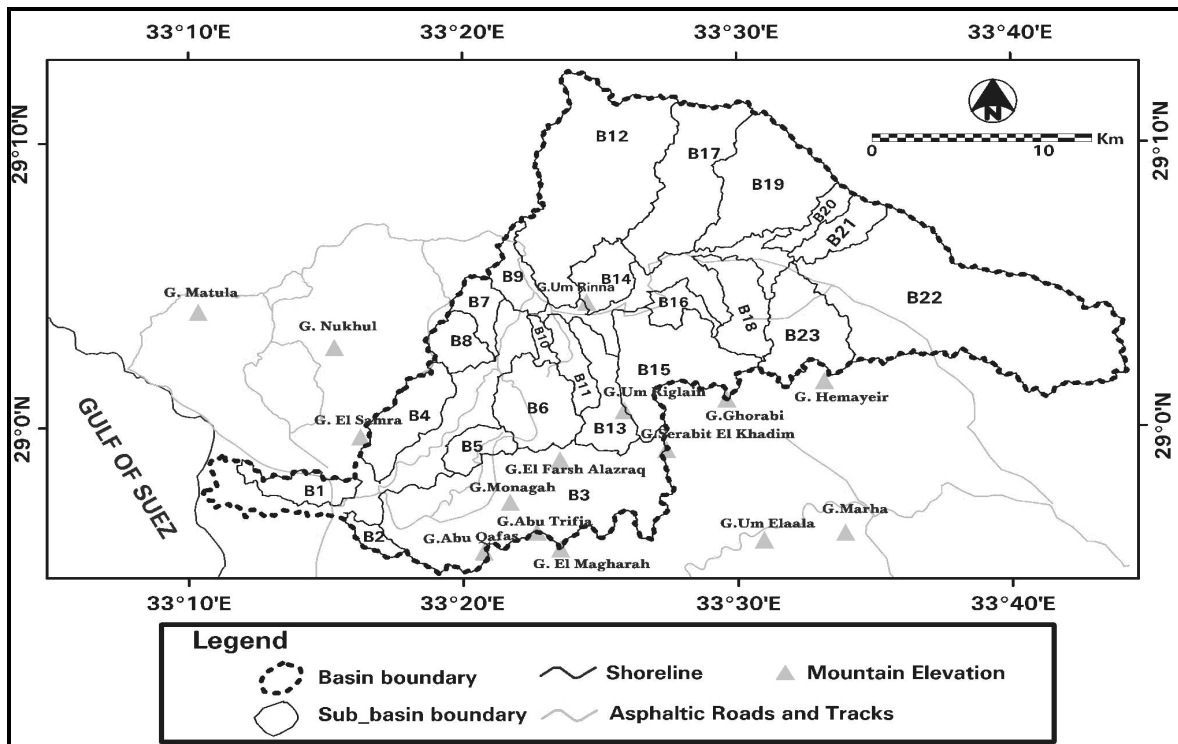


Fig. (4): Distribution of Baba basin and its sub-basins in the study area.

Table (2): Morphometric parameters of Baba basin hydrographic

Basin No.	U	N _u	L _u (km)	R _b	R _{bw}	A (km ²)	F	CD	MD	OLF	P (km)	ML (km)	Basin Shape		H (m)	MG	RF
													R _c	R _e			
B ₁	3	35	24.11	5.43	5.19	10.4	7.4	2.2	22.4	0.23	21.6	7.4	0.28	0.49	35	4.73	2.35
B ₂	3	27	8.52	3.67	3.53	4.1	4.18	3.1	12.3	0.16	11.5	4.2	0.39	0.55	34	8.13	2.31
B ₃	5	293	172.18	4.16	4.14	92.1	17.5	2.14	192.9	0.23	59.6	17.5	0.33	0.62	165	9.43	2.25
B ₄	4	67	38.92	3.94	3.88	19.4	8.73	2.23	42.4	0.22	23.3	8.7	0.45	0.57	78	8.94	2.29
B ₅	3	23	15.2	4.25	4.1	8.55	2.69	1.97	16.47	0.25	13.9	4.6	0.55	0.72	81	17.7	2.27
B ₆	4	77	44.2	3.96	3.9	23.7	6.13	2.16	50.2	0.23	22.1	6.1	0.61	0.9	87	14.2	2.25
B ₇	3	23	17.5	4.25	4.1	8.01	5.75	2.03	15.9	0.25	15.9	5.7	0.4	0.56	38	6.61	2.26
B ₈	3	34	21.4	5.25	5.1	10.1	4.15	2.2	21.6	0.23	14.3	4.1	0.61	0.86	39	9.4	2.27
B ₉	3	31	22.02	5.25	5.1	9.8	6.12	2.13	20.5	0.23	18.2	6.1	0.37	0.58	32	5.23	2.25
B ₁₀	3	10	7	2.75	2.48	3.1	3.61	2.16	6.5	0.23	10.3	3.6	0.36	0.55	17	4.71	2.25
B ₁₁	3	38	19.35	5.59	5.44	9.45	6.86	2.41	22.3	0.21	17.9	6.9	0.37	0.51	73	10.6	2.25
B ₁₂	5	271	196.02	4.13	4.11	80.84	15.4	2.2	173.9	0.23	52.96	15.5	0.36	0.66	169	10.9	2.23
B ₁₃	4	58	32.44	3.96	3.9	16.7	9.43	2.24	36.6	0.22	25.9	9.4	0.31	0.49	111	11.8	2.23
B ₁₄	4	50	26.57	3.57	4.5	12.11	5.37	2.44	28.9	0.21	16.9	5.4	0.53	0.73	33	6.14	2.23
B ₁₅	5	130	74.24	3.53	3.5	36.96	9	2.25	81.4	0.22	38.4	9	0.32	0.76	66	7.33	2.21
B ₁₆	4	31	16.3	2.73	2.64	7.12	5	2.5	17.5	0.2	18.02	5	0.28	0.6	45	8.97	2.21
B ₁₇	4	148	94.5	4.89	4.86	39.88	4.7	2.3	90.2	0.22	37.2	4.7	0.36	1.51	141	29.9	2.21
B ₁₈	4	57	42.79	3.92	3.85	16.95	8.1	2.2	36.5	0.23	24.7	8.1	0.35	0.58	45	5.57	2.19
B ₁₉	5	130	98	3.36	3.33	40.62	9.8	2.15	85.4	0.23	32.6	9.8	0.48	0.73	83	8.44	2.19
B ₂₀	3	19	16.4	4	3.79	6.72	6.5	2.02	13.3	0.25	18.1	6.5	0.26	0.45	120	18.4	2.19
B ₂₁	3	28	26.8	4.88	4.7	10.79	6.65	1.9	20.4	0.26	18.2	6.6	0.41	0.56	119	17.9	2.19
B ₂₂	5	423	294.54	4.37	4.36	118.6	21.0	2.27	263.1	0.22	62.9	21.1	0.38	0.58	135	6.4	2.13
B ₂₃	5	108	65.53	3.16	3.13	26.42	8.05	2.43	62.7	0.21	28.2	8.1	0.42	0.72	49	6.1	2.17
Baba Basin	6	2288	1544.2	4.58	4.59	688.29	3.32	2.19	1474.10	0.229	194.8	54.9	0.23	0.54	240	4.37	2.24

U = Stream order

H = Difference in elevation in meter

R_c = Circularity ratio

MD = measured stream density

R_b = Bifurcation ratioR_{bw} = Weighted mean R_b

F = Stream Frequency

N_u = Number of stream segment

RF = Rain Fall

R_e = Elongation ratio

OLF = Overland flow

ML = Max. stream Length in Km

CD = Calculated stream density

L_u = Total length of streamA = Area in Km²

P = Perimeter in Km

Table (3): The total number of streams (Nu), total stream lengths (Lu) in Km, and bifurcation ratio (Rb) in each of the drainage sub-basins and main basin of Wadi Baba

Basin code	1 st			2 nd			3 rd			4 th			5 th			6 th		
	N _u	L _u	R _b	N _u	L _u	R _b	N _u	L _u	R _b	N _u	L _u	R _b	N _u	L _u	R _b	N _u	L _u	R _b
B-1	27	10.87	7	5.99	3.9	1	7.26	7.26										
B-2	13	3.07	3	2.19	4.33	1	3.27	3.27										
B-3	233	79.42	47	46.89	4.957	10	19.67	19.7	2	13.9	5	1	12.3					
B-4	51	20.84	18	8.2	2.8	3	3.94	3.94	1	5.94	3							
B-5	18	7.91	4	3.76	4.5	1	3.54	3.54										
B-6	59	17.9	14	17.61	4.2	3	5.35	5.35	1	3.37	3							
B-7	18	7.2	4	5.35	4.5	1	4.92	4.92										
B-8	27	11.42	6	6.35	4.5	1	3.67	3.67										
B-9	26	13.2	4	6.55	6.5	1	2.27	2.27										
B-10	7	2.75	2	3.37	3.5	1	0.9	0.9										
B-11	31	10.53	6	3.21	5.2	1	5.6	5.6										
B-12	207	92.7	48	54.1	4.3	13	21.4	21.4	2	19.8	6.5	1	7.9	2				
B-13	47	16.6	8	5.5	5.9	2	2.6	2.6	1	7.8	2							
B-14	37	13.3	10	5.3	3.7	2	7	7	1	1	2							
B-15	102	37.2	21	20.3	4.9	4	7.97	7.97	2	6.85	2	1	1.98	2				
B-16	20	7.12	7	5.34	2.9	3	2.6	2.6	1	1.3	3							
B-17	114	43.5	28	24.2	4.1	5	16.6	16.6	1	10.2	5							
B-18	46	18.9	8	14.9	5.75	2	6.54	6.54	1	2.43	2							
B-19	100	45.46	22	29.2	4.5	5	15.1	15.1	2	2.3	2.5	1	5.92	2				
B-20	15	9.1	3	2.37	5	1	5	5										
B-21	23	13.55	4	8.17	5.8	1	5.1	5.1										
B-22	330	144.1	72	78.13	4.6	17	33.9	33.9	3	34.1	5.7	1	4.3	3				
B-23	82	30.6	18	18.6	4.6	5	11.4	11.4	2	3.3	2.5	1	1.64	2				
W. Baba Basin	1822	732.8	357	411.9	5.1	82	200.3	4.35	20	112.9	4.1	6	34.6	3.33	1	51.7	6	

Bifurcation Ratio (R_b) and Weighted Mean Bifurcation Ratio (R_{bw})

Generally, the theoretical minimum possible value of 2.0 is rarely approached for R_b under natural conditions (Joji and Nair 2014). Saad *et al.*, (1980) concluded that the bifurcation ratio has a relation with the geometric shape of the basin, *i.e.* (elongation and circularity) and is reflected on the rate of drainage water. Basins with high (R_b) are elongated in shape and permit the passage of runoff over an extended period of time, thus giving more chance to feed the groundwater. Whereas, basins of low (R_b) are of circular shape and allowing the surface runoff to pass in a short time forming a sharp peak. In the later case, dams should be constructed to control surface runoff. Bifurcation ratio in W. Baba basin ranges between 2.75 in W. Abu Moghirat (B-10) sub-basin and 5.59 in W. Nasib (b-11) (Table 2). In W. Baba basin, weighted mean bifurcation ratio ranges between 2.48 in W. Abu Moghirat (B10) sub-basin and 5.44 in W. Nasib (B-11) (Table 2). These values indicate the great variance between the different sub-basins in main basin. Low values indicate the increase of flash flood potentiality of the basin and minimize the chance to feed the underlying aquifers.

Drainage Frequency (F)

Quantitatively, the drainage frequency does not give direct indication to the quantity of the surface runoff (Saad *et al.*, 1980). Abdel-Mogheeth *et al.* (1985) stated that, the high value of stream frequency (more than 0.5) tend to give more possibilities for the collection of surface runoff. Drainage frequency in W. Baba basin ranges between 2.69 in W. El Homira (B-5) sub-basin and 21.06 in W. El Garf (B-22) (Table 2). These values indicate that there are great variance between the different sub-basins of the study area. Sub-basins of high stream frequency tend to have more possibilities for flood initiation.

Drainage Density (D)

It reflects the effectiveness of the overland flow as well as the infiltration and expresses the closeness of the tributaries with the basin. Also, it reflects the type of the surface layer and its relative permeability and roughness. Horton (1932) found that the mean drainage density is 0.93 km^{-1} and increases to 1.24 km^{-1} in the mountainous area with impermeable rocks having high precipitation, while it decreases in drainage basins covered by permeable rocks. Strahler (1954) stated that the basins of low drainage density are favored in regions of highly resistant or highly permeable subsoil materials under dense vegetation cover and where relief is low.

Whereas, the basins of high values are of high flash flood and favored in regions of weak or impermeable surface material, sparse vegetation and mountainous relief. Drainage density in W. Baba basin ranges between 1.9 in Tih 2 (b-21) sub-basin and 3.1 in W. Naqab Budra (b-2) sub-basin (Table 2). These values are considered high and thus reflecting the high relief, impermeable subsurface materials and sparse vegetation. It may also indicate the limited contribution of the local rainfall to groundwater and high flash flood possibility (El-Hosseiny, 2003).

Overland Flow (OLF)

Overland flow in W. Baba basin ranges between 0.16 in W. Naqab Budra (B2) sub-basin and 0.26 in Tih-2 (B21) sub-basin (Table 2). The basins of long overland flow (OLF) favours highly infiltration rate and also of low flash flooding risk.

Basin Shape

Values of circularity ratio (R_c) close to the unity indicate a nearly circular basins, while the decrease in these values indicate an increase in the elongation of the basin. Furthermore, the circularity represents the most favorable shape and conditions for the shortest runoff distance and hence, develops strong floods, while those have elongated

shape gives chances for downward infiltration and hence augmenting the existing groundwater.

Circularity Ratio (Rc) and Elongation Ratio (Re)

Circularity ratio in W. Baba basin, it ranges between 0.26 in Tih-1 (B-20) sub-basin and 0.61 in W. Abu Thor (B-6) and W. El Banat (B-8) sub-basins (Table 2). Circularity ratios near one are typical of regions of nearly circular basins with low relief and high-risk flash flood. While the low values are reflecting regions of elongation form. Elongation ratio in W. Baba basin ranges between 0.45 in W. Tih1 (B-20) sub-basin and 1.51 in W. El Rwoekta (B-17) sub-basin (Table 2). These low values are reflecting sub-basin of strong relief and steep ground slopes.

Mean Gradient (MG)

The mean gradient is obtained by dividing the difference in elevation between the source and the mouse of a basin by the length of the stream (**Taylor and Schwarz, 1952**). The slope of the basin affects mostly the quantity of infiltration that takes place and the rate of overland flow. As a result, the basins with steeper slopes allow less time for infiltration and the recharge of groundwater is minimized (**Arnous, 2016**). The mean gradient in W. Baba basin ranges between 4.71 in W. Abu Moghirate (B-10) sub-basin and 29.9 in W. El Rwoekta (B-17) sub-basin Table 2).

Flash Flooding Hazard Mapping

The terms of hazard mean a potential event that causes damage to the property. The selection of criteria that has spatial reference is an important step in decision analysis (**Malczewski, 1996; Yahaya, 2010**). Flash flood occurs when rainfall is too intense, the infiltration of the ground is low and high slope of the watershed exists. For each factor, the importance weight is defined based on its estimated significant weight numbers of the morphometric

parameters that are due to flash flood. Each factor was divided into three classes (low, moderate and high).

According to cumulative (Table 2) for the calculated morphometric parameters of all sub-basins to overview comparisons, vertically for any parameters among different sub-basins and horizontally among different parameters for any sub-basin. Based on the computed weight and mean values of the important morphometric parameters in Tables 4, sub-basins of the study area are classified into their relative amount of surface runoff, such as capability for flood hazard rank and different degrees of probability of groundwater recharge, due to different amounts infiltration within every sub-basin. The obtained results are listed in Table 4 and showing in Fig. 5.

Flash flood hazard map is established by overlaying all maps and calculation of the total weight obtained by applying ARC/INFO and using raster calculator in ARC-GIS (Fig. 5). The flood vulnerable sites have been identified and relatively categorized, risk-wise, into three ranks, namely: high, moderate and low (Fig. 5). This assortment is based on the integration of several parameters including slope gradient, basin shape, relative drainage density, overland flow, catchments area, frequency, weighted mean bifurcation ratio and average annual rainfall. **Arnous (2004) and Arnous et al. (2011)** suggested that to mitigate or at least to reduce the staggering losses and problem caused by torrential floods, the following applicable measures are recommended:

1. Construction of man-made retardation dams across the upper reaches of main wadis.
2. Digging of artificial basins at the mouth of main wadis to collect floodwater in the permeable soil of the downstream parts of main wadis.
3. Excavation of retention cisterns along the high-risk wadis.

Table (4): Flash flood hazard weight numbers of Baba Sub-basins (based on the morphometric parameters).

Basin No.	Sub-Basin Name	Flash flood scores based on								Total Hazard Score
		F	CD	A	Rc	WMPR	OLF	MG	RF	
B-01	W. Qasr El Sherif	1	3	1	3	2	1	1	3	14
B-02	W. Naqab Budra	1	1	1	2	1	3	1	3	13
B-03	W. Budra	3	3	3	3	1	1	1	2	17
B-04	W. El Samra	1	3	1	2	1	2	1	3	14
B-05	W. Homira	1	3	1	1	2	1	2	2	13
B-06	W. Abu Thor	1	3	1	1	1	1	2	2	12
B-07	W. El Kharig	1	3	1	2	2	1	1	2	13
B-08	W. El Banat	1	3	1	1	3	1	1	2	13
B-09	W. El Dabbabat	1	3	1	3	3	1	1	2	15
B-10	W. Abu Moghirat	1	3	1	3	1	1	1	2	13
B-11	W. Nasib	1	2	1	3	3	2	1	2	15
B-12	W. Ikhfi	3	3	2	3	1	1	1	2	16
B-13	W. Lehian	2	3	1	3	2	2	1	2	16
B-14	W. Um Rinna	1	2	1	1	1	2	1	2	11
B-15	W. Sewiq	2	3	1	3	1	2	1	2	15
B-16	W. Abu Maragh	1	2	1	3	1	2	1	2	13
B-17	W. El Rowekta	1	3	1	3	1	2	3	1	15
B-18	W. Um Araq	1	3	1	3	2	1	1	1	13
B-19	W. Ras Alahmar	2	3	2	2	1	1	1	1	13
B-20	W. El Tih1	1	3	1	3	2	1	2	1	14
B-21	W. El Tih2	1	3	1	2	3	1	2	1	14
B-22	W. El Garf	3	3	3	2	1	2	1	1	16
B-23	W. Hemeiyir	1	2	1	2	1	2	1	1	11

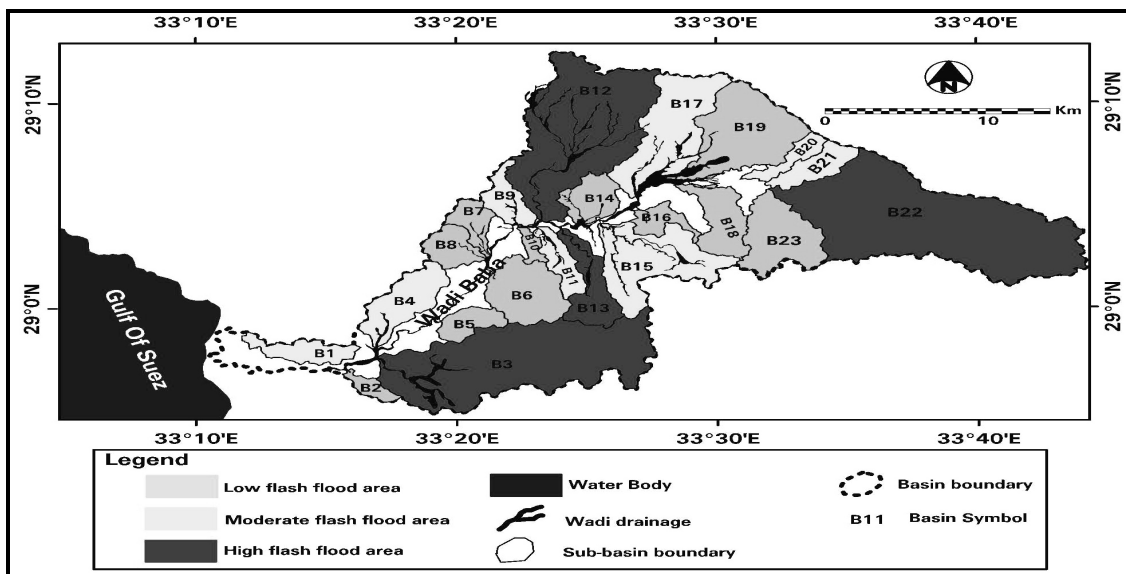


Fig. (5): Flash flood hazard map of Baba sub-basins (Based on the morphometric analysis).

Table (5): Classified sub-basins according to their flash flood hazard rank and ground water recharge probability.

Basin numbers	Ground water recharge probability	Flash flood hazard rank
B ₃ , B ₁₂ , B ₁₃ , B ₂₂	Low	High
B ₁ , B ₄ , B ₉ , B ₁₁ , B ₁₅ , B ₁₇ , B ₂₀	Moderate	Moderate
B ₂ , B ₅ , B ₆ , B ₇ , B ₈ , B ₁₀ , B ₁₄ , B ₁₆ , B ₁₈ , B ₁₉ , B ₂₃	High	Low

Conclusion

The drainage network and basin boundaries were delineated and traced on correctly enhanced satellite ASTER GDEM image by using ARC Hydro tools in Arc GIS 10.2 software. The hydrographic basin of W. Baba is divided into twenty-three sub-basins. The morphometric parameters of the drainage network were also computed by using interactivity Arc GIS 10.2 and ERDAS imagine software programs.

The morphometric parameters including; basin area (A), basin perimeter (P), stream order (U), stream number (Nu), bifurcation ratio (Rb), weighted mean bifurcation ratio (WMRb), total drainage network (Ld), basin length (L), Drainage frequency (F), drainage density (D), relief ratio (RR), drainage gradient (MG), overland flow (OLF) and basin shape (circularity ratio and elongation ratio) are calculated. Flash flood hazards in W. Baba basin is controlled by the water flowage and morphometric properties. The variation of flow is caused mainly by the morphometric parameters of the drainage basins, soil and geological characteristics, and meteorological conditions. The analysis of the various morphometric parameters of W. Baba and relating sub-basins shows that, they have different impacts on the flash flood hazards.

The most important of such parameters are the drainage frequency, drainage density, catchments area, circularity of the basin, weighted mean bifurcation ratio, overland flow, slope gradient and average annual

rainfall. Based on the computed weight and mean values of the important morphometric parameters, basins of the study area are classified into three categorized risk wise, namely: high, moderate and low flash flood hazard. The basins which have high flash flood hazard rank and low probability for ground water recharge are B₃, B₁₂, B₁₃ and B₂₂.

The present study suggests and recommends some applicable measures to mitigate or at least to reduce the staggering losses and destructions caused by torrential floods, as the construction of human retardation dams across the lower reaches of main wadi. In addition to digging of artificial basins at the mouth of W. Baba to collect floodwater in the permeable soil at the downstream parts of main wadis. Furthermore; excavation of retention cisterns along the high-risk wadis is of prime importance to reduce the destruction impacts of accumulated flood water at the downstream.

REFERENCES

- Abdel Mogheeth, S.; Abdel Daiem, A. and Hammad, F. (1985).** Hydrological remarks on Gharandal Basin, Southwest Sinai Peninsula. Desert Inst. Bull., ARE, 35: (2): 309-329.
- Abd Manap, M.; Sulaiman, W.N.A.; Ramli, M.F.; Pradhan, B. and Surip N. (2013).** A knowledge-driven GIS modeling technique for groundwater potential mapping at the Upper Langat

- Basin, Malaysia. *Arabian J. Geosci.*, 6 (5): 1621–1637.
- Aggour, T.A. and Gomaa, M.A. (2008).** Hydrogeological and hydrogeochemical studies in Wadi Baba and Sidri, Southwestern part of Sinai, Egypt. *Annals Geol. Surv. Egypt.* xxx: 497-528.
- Aglan, O.S. (1995).** Geology of groundwater supplies in the area between Wadi Gharandal and Wadi Sidri, Southwestern Sinai. MSc. Thesis, Dept. Geol., Fac. Sci., Ain Shams Univ., 202.
- Al-Harhi, A.A. (2003).** Assessment of flooding hazards at Al-Lith area, West Saudi Arabia. *Annals Geol. Surv. Egypt*, V.XXVI, 529-551.
- Arnous, M.O. (2011).** Integrated remote sensing and GIS techniques for landslide hazard zonation: a case study Wadi Watier area, South Sinai, Egypt. *J. Coast Conserv*, 15 (4): 477–497, DOI 10.1007/s11852-010-0137-9.
- Arnous, M.O. (2016).** Groundwater potentiality mapping of hard-rock terrain in arid regions using geospatial modelling: example from Wadi Feiran basin, South Sinai, Egypt. *Hydrogeol. J.*, 24 (6): 1375–1392. doi: 10.1007 /s 10040- 016-1417-8
- Arnous, M.O.; Aboulela, H.A. and Green, D.R. (2011).** Geo-environmental hazards assessment of the north western Gulf of Suez, Egypt. *J Coast Conserv* 15(1):37 – 50. doi: 10.1007/s11852-010-0118-z.
- Arnous, M.O.; El-Rayes, A.E. and Green D.R. (2015).** Hydrosalinity and environmental land degradation assessment of the East Nile Delta region, Egypt. *J. Coast Conserv.*, 19 (4): 491–513. doi:10.1007/s11852-015-0402-z.
- Arnous, M.O. and Green, D.R. (2011).** GIS and remote sensing as tools for conducting geo-hazards risk assessment along Gulf of Aqaba coastal zone, Egypt. *J. Coast Conserv.*, 15 (4): 457–475. doi:10.1007/s11852-010-0136-x
- Arnous, M.O. and Green, D.R. (2015).** Monitoring and assessing water-logged and salt-affected areas in the Eastern Nile Delta region, Egypt, using remotely sensed multi-temporal data and GIS. *J. Coast Conserv.*, 19 (3): 369–391, doi: 10.1007/s11852-015-0397-5.
- Arnous, M.O. (2004).** Geo-environmental assessment of Cairo-Ismailia road area, Egypt, using remote sensing and geographic information system (GIS). Ph.D. Thesis, Geol. Dept., Fac. Sci., Suez Canal Univ., Ismailia, 283.
- Bajabaa, S.; Masoud, M. and Al-Amri, N. (2014).** Flash flood hazard mapping based on quantitative hydrology, geomorphology and GIS techniques (case study of Wadi Al Lith, Saudi Arabia). *Arab J. Geosci.*, 7 : 2469–2481, DOI 10.1007/s12517-013-0941-2.
- Ball J. (1916). The geography and geology of west central Sinai, Egypt. *Surv. Dept.*, Cairo, p 219.
- Bapalu, V.G. and Sinha, R. (2005).** GIS in flood hazard mapping: A case study of Kosi River Basin, India. www.gisdevelopment.net, Natural Hazard Management, ESRI.
- Be'eri-Shlevin, Y.; Katzir, Y. and Whitehouse, M. (2009).** Postcollisional tectono-magmatic evolution in the northern Arabian-Nubian Shield (ANS) time constraints from ionprobe U–Pb dating of zircon. *Journal of Geological Society (London)*, 166: 71–85.
- CEOS (2003).** the use of earth observing satellites for hazard support: assessments and scenarios. Final report of the CEOS Disaster Management Support Group (DMSG). Helen M. Wood, Chair. National Oceanic and Atmospheric Administration (NOAA) United States Department of Commerce.

- Climatic Atlas of Egypt (1996).** Ministry of transport and communications, Egyptian Meteorological Authority, Cairo, Egypt.
- Climatological Normals of The Arab Republic of Egypt (1980).** Climatological Normals for the Arab Republic of Egypt up to 1975. Ministry of Civil Aviation, Egypt. Meteorol. Authority, Cairo, Egypt.
- El-Baz, F. (1995).** Utilizing satellite images for groundwater exploration in fracture zone aquifers. Water resources management in arid condition, Muscal, Sultanate of Oman, 419-427.
- El-Shamy, I.Z. (1983).** On the hydrogeology of west Central Sinai. Egypt. J. Geol., 27 (1-2): 93-105.
- El-Hosseiny, M.S. (2003).** Geophysical and hydrogeological studies on El-Ain El-Sokhan industrial area, Egypt. M.Sc. Thesis, Dept. Geol., Fac. Sci., Fayoum Univ., Egypt.
- El-Rayes, A.E. and Arnous, M.O. (2015).** A novel approach in hydrogeochemical exploration for uranium mineralization: example from west central Sinai, Egypt. Acta Geol. Sinica (English Ed.), 89 (6): 1895–11913. doi: 10.1111/1755-6724.12606.
- El-Rayes, A.E.; Arnous, M.O. and Aboulela, H.A. (2015).** Hydrogeochemical and seismological exploration for geothermal resources in South Sinai, Egypt utilizing GIS and remote sensing. Arab J. Geosci., 8 (8): 5631–5647. doi: 10.1007/s12517-014-1667-5.
- Eyal, M.; Litvinovsky, B.; Jahn, B.M.; Zandvilevich, A. and Katzir, Y. (2010).** Origin and evolution of post-collisional magmatism: Coeval Neoproterozoic calc-alkaline and alkaline suites of the Sinai Peninsula. Chem. Geol., 269 (3–4): 153–179.
- Fernandez, D. and Lutz, M. (2010).** Urban flood hazard zoning in Tucumán Province, Argentina, using GIS and multicriteria decision analysis. Eng. Geol., 111 (1–4): 90–99.
- Gardiner, V. (1990).** Drainage basin morphometry. In: Goudie A (ed) Geomorphological techniques. Unwin Hyman, London, 71–81.
- Hammad, F.A. (1980).** Geomorphological and hydrological aspects of Sinai Peninsula, A.R.E. Geol. Surv. Egypt., 10: 807-817.
- Hammad, F.A. and Misak R.F. (1985).** Quantitative geomorphology and groundwater possibilities in the vicinities of Wadi Nasib, Abu Zeneima, Sinai, Egypt. Des. Inst. Bull. ARE, 35 (2): 331-351.
- Horton, R.F. (1932).** Drainage basin characteristics, Trans. An., Geophys. Union, 13: 350-361.
- Horton, R.F. (1945).** Erosional development of streams and their drainage basins. Hydrophysical approach to quantitative morphology. Bull. Geol. Soc. Ame., 56: 275-370.
- Joji, V.S. and Nair, A.S.K. (2014).** Terrain characteristics and longitudinal, land use and land cover profiles behavior—a case study from Vamanapuram river basin, southern Kerala, India. Arab. J. Geosci., 7 (4): 1351–1361, doi:10.1007/s12517-012-0815-z.
- Kumar, R.; Kumar, S.; Lohani, A.K.; Nema, R.K. and Singh, R.D. (2000).** Evaluation of geomorphological characteristics of a catchment using GIS. GIS India, 9 (3): 13-17.
- Maidment, D.R. (2002).** ArcHydro GIS for water resources. California: ESRI Press.
- Malczewski, J. (1996).** A GIS-based approach to multiple criteria group decision making. Int. J. Geographic Information System, 10 (8): 955-971.
- Martz, L.W. and Garbrechet, J. (1992).** Numerical definition of drainage

- network and sub catchment areas from digital elevation models, *Computer Geosci.*, 18 (6): 747–761.
- Mondal, T. and Gupta, S. (2015).** Evaluation of morphometric parameters of drainage networks derived from topographic map and digital elevation model using remote sensing and GIS. *Int. J. Geom. and Geosci.*, 5 (4): 655-664.
- Nageswararao, K.; Swarna, L.P.; Arun, K.P. and Hari, K.M. (2010).** Morphometric analysis of Gostani River Basin in Andhra Pradesh State, India using spatial information technology. *Int. J. Geom. Geosci.*, 1(2):79–187.
- Omran, A.; Schroder, D.; El-Rayes, A. and Geriesh, M. (2011).** Flood hazard assessment in Wadi Dahab, Egypt based on basin morphometry using GIS techniques. *GI-Forwm 11, Geoinformatics Forum Salzburg, Aust.*
- Patton, C. (1988).** Drainage basin morphometry and floods. In: Baker VR *et al* (eds) *Flood geomorphology*. Wiley, New York, 51–65.
- Rai, P.K.; Mohan, K.; Mishra, S.; Ahmed, A. and Mishra, V.N. (2014).** A GIS-based approach in drainage morphometric analysis of Kanhar River Basin, India. *Appl Water Sci*, doi:10.1007/s13201-014-0238-y.
- Saad, K.F.; El-Shamy, I.Z. and Sweidan, A.S. (1980).** Quantitative analysis of geomorphology and hydrology of Sinai Peninsula. 5th Afr. Conf., ARE.
- Shata, A.A. (1955).** Some remarks on the distribution of the Carboniferous formations in Egypt. *Bull. Inst. Des. Egypt.*, 5: 241-247.
- Strahler, A.N. (1954).** Quantitative geomorphology of erosional landscapes, C. R. 19th Intern. Geol. Cong., Algiers, 1952, Sec., 13 (3): 341-354.
- Strahler, A.N. (1964).** Quantitative geomorphology of drainage basins and channel networks. In: *Handbook of Appl. Hydrol.* New York: McGraw Hill Book Company, Section 4II.
- Subyani, A.M. (2011).** Hydrologic behavior and flood probability for selected arid basins in Makkah area, western Saudi Arabia. *Arab. J. Geosci.*, 4 (5): 817-824, doi:10.1007/s12517-009-0098-1.
- Taylor, A.B. and Schwarz, E. (1952).** Unit hydrograph lag and peak flow related to basin characteristics. *Transactions of the Ame. Geophysical Union*, 235-246.
- Yahaya, S. (2010).** Multicriteria Analysis for Flood Vulnerable Areas in Hadejia-Jama'are River Basin, Nigeria. *Europ. J. Sci. Res.*, 1450216X, 20100501.
- Zerger, A. and Smith, D.I. (2003).** Impediments to using GIS for real-time disaster decision support. *Comp Environ. Urban Sys*, 27:123–141.
- Zhang, X.U.; Zhou, T. and Zheng, J. (2009).** DEM-based spatial discretization and parameter database design for distributed hydrological model. *Proc. SPIE 7498, MIPPR 2009: Remote Sensing and GIS Data Processing and Other Applications*, 749831 (October 30, 2009); doi:10.1117/12.832487.

المخلص العربي

تخطيط مخاطر السيول في وادي بعبع، جنوب غرب سيناء، مصر

على السيد على عمر^١، محمد عثمان عرنوس^٢، محمد الغوايبي^٢،عبدالله سليمان الشامى^١، محمد على الزلقى^١

١- قسم الجيولوجيا والاستشعار عن بُعد، هيئة المواد النووية، القاهرة، مصر.

٢- قسم الجيولوجيا، كلية العلوم، جامعة قناة السويس، مصر.

مخاطر السيول في المنطقة الجبلية جنوب غرب سيناء تتطلب معلومات موثوقة ودقيقة. هذه المخاطر هي الأخطر بشكل رئيسي لذلك تم اسقاط الضوء عليها وابرزها من خلال هذا العمل لأنها تهدد حياة الناس وتعوق أي تخطيط للتنمية المستدامة في المناطق ذات الطوبوغرافية الوعرة وما حولها. وتهدف الدراسة الحالية إلى تطبيق نظم المعلومات الجغرافية والاستشعار عن بعد لبناء خريطة مخاطر السيول استنادا إلى المعلومات الجيومورفومترية المستخرجة من نموذج الارتفاع الرقمي (DEM) وتقييم رتبة خطر السيول لحوض وادي بعبع وأحواضه الفرعية، وادي بعبع يقع في منطقة قاحلة ويعتبر حوض كبير في منطقة الدراسة جنوب غرب سيناء التي تصب في خليج السويس، أيضاً تم تحديد و تتبع شبكات الصرف وحدود الحوض وتم حساب المعلومات المورفولوجية لشبكات الصرف لحوض وادي بعبع، ومن الواضح أن شدة السيول محكومة بشكل رئيسي بقيم المعلومات الجيومورفومترية والترتبة والخصائص الجيولوجية، وظروف الأرصاد الجوية، لذلك تم تقسيم أحواض الصرف الفرعية لوادي بعبع إلى ثلاث رتب وهم عالية ومتوسطة ومنخفضة وتم عمل خريطة للنطاقات المعرضة للسيول والفيضانات بناء على نتائج تحاليل احواض الصرف بوادي بعبع و حساب الاوزان التقديرية لها وحساب الجمع الجبرى لهذه الاوزان وجد ان الأحواض الفرعية لحوض وادي بعبع التي تحمل الرموز الآتية ($B_3, B_{12}, B_{13}, B_{22}$) ذات مخاطر السيول المرتفعة مع احتمال ضئيل لتغذية المياه الجوفية.

الكلمات الإسترشادية: تخطيط، مخاطر السيول، وادي بعبع، جنوب غرب سيناء، مصر.

المحكمون:

١- أستاذ الهيدرولوجيا، كلية العلوم، جامعة قناة السويس، مصر.
 ٢- أستاذ الجغرافيا المساعد، كلية الآداب، جامعة العريش، مصر.

١- أ.د. أحمد السيد الرئيس
 ٢- د. محمد فؤاد عبد العزيز

